Integrity risk of cycle resolution in the presence of bounded faults

Samer Khanafseh, Mathieu Joerger, and Boris Pervan
Illinois Institute of Technology
Chicago, IL

Abstract— **This paper introduces a method to compute an upper bound on the integrity risk of cycle resolution in the presence of bounded measurement errors and faults. In high accuracy applications such as shipboard landing and autonomous airborne refueling, carrier phase cycle ambiguities must be estimated and resolved as integers (or 'fixed ambiguities'). In applications that also demand high integrity, the cycle resolution process must comply with a fault-free integrity risk requirement. Under normal error conditions, fault-free integrity risk can readily be quantified using existing cycle resolution methods; this is true even in the presence of known measurement biases. However, evaluating the integrity risk of a cycle resolution process under fault hypotheses has not yet been addressed. In the case of rare-event measurement faults such as satellite failures and atmospheric anomalies, the magnitude of the fault is never exactly known, but it can often be bounded. The bound can either be a result of a monitor's minimum detectable error, from extensive data analysis, or even from physical limitation. In this paper, we develop a method to account for these bounded errors in the computation of the integrity risk for navigation systems that rely on fixed carrier phase cycle ambiguities.**

Keywords-component; Cycle Resolution; Integrity Risk; Bounded faults.

I. INTRODUCTION

The fault-free integrity risk is typically defined as the probability that the position error exceeds predefined alert limits. In applications where integrity and accuracy requirements are stringent, it is necessary to quantify the impact of the cycle resolution process on position domain integrity. In this context, the bootstrap fixing method is used as a baseline for cycle resolution because it provides an *a priori* success rate (probability of correct fix and probability of incorrect fix). Using these probabilities, several simple methods can then be used to evaluate the fault free integrity risk of cycle resolution processes by only considering the correct fixes. But these methods are conservative because they assume that all incorrect fixes result in a position estimate error that exceeds the requirements. In recent years, new methods have been developed to compute the fault free integrity risk of cycle resolution methods by also evaluating the impact of incorrect fixes on the position estimates. Examples of such algorithms are the Enforced Position-domain Integrity-risk of Cycle resolution (EPIC) method [1], and the Geometric Extra Redundancy Almost Fixed Solution (GERAFS) method [2].

Two separate types of probabilities must be calculated when evaluating the integrity risk of cycle resolution. The first is the probability of correct fix (and probability of incorrect fix for the EPIC and GERAFS methods). The second probability is computed from the conditional distribution of the position estimate error for the fixed solution. Both of these probability types are strongly influenced by rare-event measurement faults. Several publications address computing the probability of correct fix in the presence of measurement biases (for example, see [3]). However, these methods are only applicable if the bias on the measurement error is exactly known. In reality, the magnitude of ranging measurement faults is rarely, if ever, known, but in some cases the magnitude of the faults can be bounded. Unfortunately, it can be shown that simply using measurement bounds in place of the exact biases required by the existing methods does not provide bounding integrity risk probabilities.

Two examples of unknown, but bounded, measurement errors and faults can be presented. First, the impact of satellite failures such as orbit ephemeris faults can be mitigated by external measurement monitoring. In this case, the fault magnitude is limited by the monitor's minimum detectable error (MDE), which is the smallest fault that the monitor is able to detect given an allocated integrity risk requirement [4]. In order to quantify the overall integrity risk of the user position solution, the MDE can be exploited as a bound on the measurement fault. Second, in the case of faults that are difficult to monitor, such as tropospheric anomalies, measurement error bounds can be established by exhaustive data analysis and possibly even physical limits [5]. In this paper, we derive a method to use these measurement error and fault bounds to establish a bound on the probability of correct fix, on the probability of incorrect fixes, and on the position estimate error after fixing. A tight bound on the integrity risk can then be computed using these bounded probabilities.

In order to verify the developed approaches in this work in providing bounds on the integrity risk, Monte-Carlo simulations are carried out for two cycle resolution methods: conventional bootstrap method and EPIC. In these simulations, different fault magnitudes are injected to the measurements while only the known bound on these errors is used in the computation of integrity risk. Furthermore, we quantify the performance of the integrity risk bounding methods, as measured by availability, on an example autonomous shipboard landing application. In this analysis we consider tropospheric

The authors gratefully acknowledge the Naval Air Systems Command (NAVAIR) of the US Navy for supporting this research.

anomalies as the source of bounded error, where extensive data is used to establish the bound.

II. Integrity Risk of Cycle Resolution

Different methods have been developed to address the issue of the integrity of cycle resolution. Although certain methods, such as the ratio test, provide a measure of the quality of cycle resolution, it is not yet clear how to tie such a test to the integrity risk requirements [6] and [7]. Other methods such as [8] provide a probabilistic measure of the ambiguity resolution that can be used for integrity verification. However, this method provides an *a posteriori* measure and depends on access to the measurements. The bootstrap method, on the other hand, provides an *a priori* measure of the probability of correct cycle ambiguity estimation. Furthermore, since this probability was derived stochastically, it is easily implementable in applications with integrity risk requirements. Therefore, in this section we briefly describe two approaches to address the integrity of cycle resolution using the bootstrap fixing method: a *conventional method* and *EPIC*.

A. Conventional Method

This section briefly summarizes the method derived in [9], which we refer to here as the "*conventional method*". It provides a formula relating the probability of incorrect fix P_{IF} threshold, the fault-free integrity risk requirement (I_{H0req}) and the vertical protection level. To derive the formula, it is easiest to start with the concept of the fault free Vertical Protection Level (VPL_{H0}). VPL_{H0} is defined in (1) as a statistical overbound such that the probability of the vertical position estimate error ($|\hat{x}_v - x_v|$) exceeding VPL_{H0} equals $I_{H0\,req}$.

$$P\{|\hat{x}_v - x_v| > VPL_{H0}\} = I_{H0req} \tag{1}$$

where,

P{■}: the probability of event '■'

$\hat{x}_v$: vertical component of the estimated relative position vector

x_v: vertical component of the true relative position vector

After fixing the ambiguities, two mutually exclusive and exhaustive events can be defined in relation to (1): a *correct fix* (CF) and an *incorrect fix* (IF) event. An IF includes all events where some or all ambiguities have been fixed incorrectly. A CF, on the other hand, includes only those events where no ambiguities are fixed incorrectly. Note that by definition of a correct fix, if we choose not to fix any ambiguity, thereby leaving the cycle ambiguities floating, then the Probability of Correct Fix (P_{CF}) is equal to 1. At the same time, if we choose to fix some or all ambiguities, we expect P_{CF} to be less than 1. Using the law of total probability, (1) can be expanded to,

$$\begin{aligned} P\{|\hat{x}_v - x_v| > VPL_{H0}\} = {} & P\{|\hat{x}_v - x_v| > VPL_{H0} | CF\} P_{CF} \\ & + P\{|\hat{x}_v - x_v| > VPL_{H0} | IF\} P_{IF} \end{aligned} \tag{2}$$

In this method, the probability that the vertical error exceeds VPL_{H0} given that the cycle ambiguities are fixed incorrectly (i.e., $P\{|\hat{x}_v - x_v| > VPL_{H0} | IF\}$) is conservatively assumed to be equal to 1. This assumption is considered conservative because in reality there might be incorrect fix events that result in a small vertical error such that $P\{|\hat{x}_v - x_v| > VPL_{H0} | IF\}$ is less than 1.

Since the correct fix and incorrect fix events are mutually exclusive and exhaustive, as defined earlier, $P_{CF} = 1 - P_{IF}$. Using the conservative assumption $P\{|\hat{x}_v - x_v| > VPL_{H0} | IF\} = 1$ in (2) and substituting the result in (1),

$$I_{H0req} = P\{|\hat{x}_v - x_v| > VPL_{H0} | CF\} P_{CF} + P_{IF} \tag{3}$$

or equivalently,

$$P\{|\hat{x}_v - x_v| > VPL_{H0} | CF\} = \frac{I_{H0req} - P_{IF}}{1 - P_{IF}} \tag{4}$$

Under the assumption that the GPS measurement noise is bounded by a zero-mean Gaussian distribution, the vertical position error after fixing the cycle ambiguities correctly can be assumed to be a random variable with a Gaussian distribution of zero mean and standard deviation $\sigma_{v|CF}$. Therefore, a probability multiplier ($K_{VPL|CF}$) is calculated using the inverse of the cumulative normal distribution function of $P\{|\hat{x}_v - x_v| > VPL_{H0} | CF\}$. For example, for $I_{H0\,req} = 10^{-7}$, in [9] a reasonable threshold for P_{IF} for some aircraft navigation applications was found to be 10^{-8}, which results in $K_{VPL|CF} = 5.35$. During a typical navigation operation, only a subset of ambiguities (or linear combinations thereof) can be fixed with a joint incorrect fix probability lower than the threshold P_{IF}. The rest of the ambiguities must be left as floating numbers. This set of partially fixed ambiguities is then used in position estimation and to generate $\sigma_{v|CF}$. VPL_{H0} is then calculated by multiplying $\sigma_{v|CF}$ by 5.35. This VPL_{H0} must comply with the maximum tolerable vertical error, which is known as the Vertical Alert Limit (*VAL*).

Using this method, fixing a sufficient number of ambiguities to meet the tight accuracy requirement with a success rate that meets the integrity risk requirement is not always possible [10,11]. Therefore, if a tight accuracy and integrity requirements exist, as we will encounter later, this method is not sufficient to provide reasonable navigation availability. One venue to improve the VPL_{H0} calculation is the conservative assumption, made after (2), that all incorrect integer candidates will cause the position errors to exceed the alert limits. This assumption was eliminated in the development of EPIC [1].

B. EPIC Algorithm

Instead of using the conservative assumption that the vertical error exceeds VPL_{H0} if ambiguities are fixed incorrectly, EPIC considers an integer space that includes all candidate sets of cycle ambiguities that cause the position error to fall inside the alert limit boundaries. This includes all sets, correct or incorrect fixes, as long as they cause the vertical error to be bounded by the alert limits with the allowable level

of integrity risk. In other words, if a candidate set is incorrect but satisfies the position domain alert limit constraints, we recognize that it does not violate integrity. In the remainder of this section, we briefly explain the EPIC algorithm. For more details, see [1].

Although VPL can be computed in EPIC [1], it is easier to derive it and implement it by computing integrity risk directly. Instead of starting from the definition of VPL_{H0} that meets the integrity requirements, EPIC calculates the integrity risk (I_{H0}) induced by the cycle ambiguity candidates and compares it to the required fault free integrity risk (I_{H0req}). If the calculated integrity risk (I_{H0}) is less than the required integrity risk then the navigation system is considered available under fault-free conditions. Fault free integrity risk is defined as the probability that the vertical error exceeds *VAL* as shown in (5).

$$I_{H0} = P\left\{\left|\hat{x}_v - x_v\right| > VAL\right\} \tag{5}$$

Considering the mutually exclusive and exhaustive events corresponding to *CF* and all possible incorrect fixes IF_k and using the law of total probability, (5) can be rewritten as

$$\begin{aligned} I_{H0} = {} & P\left\{\left|\hat{x}_v - x_v\right| > VAL \mid CF\right\}P_{CF} \\ & + \sum_{k=1}^{\infty} P\left\{\left|\hat{x}_v - x_v\right| > VAL \mid IF_k\right\}P_{IFk} \end{aligned} \tag{6}$$

where,

IF_k: event corresponding to the k^{th} incorrectly fixed cycle ambiguity vector

P_{IFk}: probability of occurrence of the k^{th} incorrect fix

Since it is impractical to calculate the series with an infinite number of incorrect cycle ambiguity vector candidates, the series is broken into two subseries: one represents what will later be the candidates of interest ($k = 1 \rightarrow l$) and another which includes all remaining candidates ($k = l + 1 \rightarrow \infty$). In order to avoid calculating the latter subseries the conservative assumption $P\left\{\left|\hat{x}_v - x_v\right| > VAL \mid IF_k\right\} = 1$ for $k = l + 1 \rightarrow \infty$ is used. Using the fact that the correct fix and all incorrect fix events are mutually exclusive and exhaustive and then simplifying and rearranging the resultant equation yields

$$\begin{aligned} I_{H0} = {} & 1 - \left(1 - P\left\{\left|\hat{x}_v - x_v\right| > VAL \mid CF\right\}\right)P_{CF} \\ & - \sum_{k=1}^{l}\left(1 - P\left\{\left|\hat{x}_v - x_v\right| > VAL \mid IF_k\right\}\right)P_{IFk} \end{aligned} \tag{7}$$

In [1], it has also been shown that similar expressions to (7) can be written for requirements other than *VAL*, such as Lateral Alert Limit (*LAL*), vertical accuracy or lateral accuracy.

Equation (7) is a closed-form expression in which the effect of a set of ambiguity candidates on the position domain integrity risk is explicitly defined. In [1] it was shown that if the series term in (7) (which represents the incorrect fix candidates to be tested) is neglected, the remaining expression yields an equivalent representation to (3) with *VAL* and I_{H0} replacing VPL_{H0} and I_{H0req}, respectively. Therefore, as long as the sum of the series in (7) is greater than zero (which is always true), the integrity risk computed using (7) will be lower than that given by the conventional method. Therefore, the EPIC algorithm portrayed in equation (7) provides a tighter bound on integrity risk than the conventional method. This in turn results in improved navigation availability as shown in [1] and as we will show in the results section.

An efficient method that is based on a sequential elimination procedure has been developed and detailed in [1] to construct the best cycle ambiguity candidates to be considered in (7). For compactness of notation, we will refer to $P\left\{\left|\hat{x}_v - x_v\right| > VAL \mid CF\right\}$ and $P\left\{\left|\hat{x}_v - x_v\right| > VAL \mid IF_k\right\}$ as $P_{VAL|CF}$, and $P_{VAL|IFk}$, respectively. Although the details of how to compute these quantities can be found in [1], we will discuss briefly their computation because we will use it later in the integrity risk bounding section.

Calculating the probability that a set of ambiguities is the correct one depends on the fixing method utilized. In this work, the bootstrap method [12] is used for cycle resolution because it provides a closed form *a priori* probability mass function of the integer estimation error. The bootstrap rounding method fixes ambiguities sequentially and provides a measure of P_{CF} at each step of the fixing process. The sequential adjustment is performed according to the cycle ambiguity conditional variances with the ambiguity having the lowest conditional variance being fixed first. The i^{th} conditional variance ($\sigma^2_{i|I}$), defined as the variance of the ambiguity i conditioned on the previous ambiguities in the set $I = \{1,2,\ldots,i\text{-}1\}$ being fixed, is the (i,i) element of the diagonal matrix **D** resulting from the $\mathbf{LDL}^{\mathrm{T}}$ decomposition of the decorrelated floating cycle ambiguity estimate error covariance matrix. At each step in this sequence (the m^{th} step for example), the probability of the bootstrapped integer estimate ($\breve{\mathbf{a}}$) (which is an $m \times 1$ vector) being any arbitrary integer candidate (**n**) given that the correct fixed ambiguity is (**a**), is given in [12] as,

$$\begin{aligned} P\left(\breve{\mathbf{a}} = \mathbf{n}\right) = \prod_{i=1}^{m}\Bigg[& \Phi\left(\frac{1 - 2\mathbf{l}_i^T\left(\mathbf{a} - \mathbf{n}\right)}{2\sigma_{i|I}}\right) \\ & + \Phi\left(\frac{1 + 2\mathbf{l}_i^T\left(\mathbf{a} - \mathbf{n}\right)}{2\sigma_{i|I}}\right) - 1\Bigg] \end{aligned} \tag{8}$$

where,

$\mathbf{l}_i$: the i^{th} column vector of the unit lower triangular matrix ($\mathbf{L}^{-\mathrm{T}}$) resulting from $\mathbf{LDL}^{\mathrm{T}}$ decomposition of the ambiguity covariance matrix

m: the number of cycle ambiguities fixed $m \le n$

and $\Phi(x) = \int_{-\infty}^{x} \frac{1}{\sqrt{2\pi}} \exp\left(-\frac{1}{2}v^2\right) dv$

Therefore, if we set **n** equal to **a** (the correct cycle ambiguity vector), Equation (8) produces

$$P\left(\breve{\mathbf{a}} = \mathbf{a}\right) = \prod_{i=1}^{m}\left[2\Phi\left(\frac{1}{2\sigma_{i|I}}\right) - 1\right] \tag{9}$$

which can be used to calculate P_{CF}. For P_{IF}, the value of $(\mathbf{a} - \mathbf{n})$ can be computed for the incorrect fix candidate of interest. For example, if a one cycle error on the first ambiguity is to be used as the first incorrect fix event (IF_1), then the vector $[1\ 0 \ldots 0]^T$ is used for $(\mathbf{a} - \mathbf{n})$ in calculating P_{IF1}.

Before estimating the probability of the vertical error exceeding *VAL*, for simplification in notation, the conditional events *CF* and IF_k are replaced by a general event *D*. Later on, when we derive a methodology for estimating this probability, we will tackle the difference between the *CF* and *IF* events and discuss the specific approach for each one. By expanding the absolute value inside the conditional probability term of (7), the probability of the vertical error exceeding *VAL* given that event *D* took place can be written as:

$$\begin{aligned} P\{|\hat{x}_v - x_v| > VAL \mid D\} = P\{(\hat{x}_v - x_v) < -VAL \mid D\} \\ + P\{(\hat{x}_v - x_v) > VAL \mid D\} \end{aligned} \quad (10)$$

The position vector is linearly estimated using GPS measurements with errors that are assumed to be bounded by Gaussian distributions with zero mean. Therefore, the distribution of the vertical position estimate error will also be Gaussian with a standard deviation defined as $\sigma_{v|D}$. The mean of this distribution will depend on the event *D* and hence is referred to as μ_D. Knowing the mean (μ_D) and the standard deviation ($\sigma_{v|D}$), the probability of the first and second terms of the right hand side in (10) can be calculated using the normal cumulative distribution function at the limits -*VAL* and *VAL*, respectively.

Returning to the *CF* and IF_k events, the standard deviation of the vertical position error is not affected by an incorrect fix. Therefore, $\sigma_{v|D} = \sigma_{v|CF}$ for both the *CF* and IF_k events (the calculation of $\sigma_{v|CF}$ is detailed below). The only difference between these events is the mean of the Gaussian distribution. Since the position vector is estimated using unbiased estimators (such as least squares or Kalman filter estimators), the mean is zero ($\mu_{CF} = 0$) for the *CF* event (P_{VALCF}). In the case of IF_k events, the incorrect integer candidate will induce a bias in the relative position vector estimate. The resulting position domain bias caused by the k^{th} incorrect candidate $(\mathbf{a} - \mathbf{n})_k$ depends on the estimator used. Next, a method to compute $\sigma_{v|CF}$ and the bias for an example Kalman filter implementation is detailed. A similar procedure can be followed to derive $\sigma_{v|CF}$ and the bias for other estimators. $P_{VAL|IFk}$ can then be calculated using a normal cumulative distribution function with standard deviation $\sigma = \sigma_{v|CF}$ and a mean (μ_{IFk}) equal to the vertical component of the position domain bias.

Assume that prior to the fixing step, the state estimate $\hat{\mathbf{s}}$, vector containing the floating cycle ambiguities and the relative position vector, and the associated estimate error covariance $\hat{\mathbf{P}}$ are expressed as, $\hat{\mathbf{s}} = \begin{bmatrix} \hat{\mathbf{x}}_{3\times 1} \\ \hat{\mathbf{a}}_{n\times 1} \end{bmatrix}$ and $\hat{\mathbf{P}} = \begin{bmatrix} \mathbf{P}_{\hat{\mathbf{x}}} & \mathbf{P}_{\hat{\mathbf{x}}\hat{\mathbf{a}}} \\ \mathbf{P}_{\hat{\mathbf{a}}\hat{\mathbf{x}}} & \mathbf{P}_{\hat{\mathbf{a}}} \end{bmatrix}$. In this section, integer fixing is performed one ambiguity at a time, with an integrity check before fixing a subsequent cycle ambiguity. That is, we only fix the next ambiguity if the fixing operation does not violate the integrity risk requirement. If the LAMBDA decorrelation scheme is used [13], the i^{th} ambiguity in the Z-decorrelated space $\hat{a}_z^{(i)}$ is rounded to its nearest integer $\breve{a}_z^{(i)}$.

$$\breve{a}_z^{(i)} = \text{round}\left(\begin{bmatrix} \mathbf{0}_{1\times 3} & \mathbf{Z}_i \end{bmatrix} \breve{\mathbf{s}}^{(i-1)} \right) \quad (11)$$

where,

$\breve{a}_z^{(i)}$: i^{th} rounded ambiguity element

$\mathbf{Z}_i$: i^{th} row of the transformation matrix $\mathbf{Z}$. Notice, however, that if the LAMBDA decorrelation is not used, $\mathbf{Z} = \mathbf{I}$

$\breve{\mathbf{s}}^{(i-1)}$: updated state vector $\mathbf{s}$ based on fixing ambiguities 1 to $i-1$, such that $\breve{\mathbf{s}}^{(0)} = \hat{\mathbf{s}} = \begin{bmatrix} \hat{\mathbf{x}}^T & \hat{\mathbf{a}}^T \end{bmatrix}^T$.

Next, the position state vector estimate and remaining floating ambiguities $\breve{\mathbf{s}}$ are updated accordingly as follows:

$$\mathbf{K} = \breve{\mathbf{P}}^{(i-1)} \begin{bmatrix} \mathbf{0}_{1\times 3} & \mathbf{Z}_i \end{bmatrix}^T \left(\begin{bmatrix} \mathbf{0}_{1\times 3} & \mathbf{Z}_i \end{bmatrix} \breve{\mathbf{P}}^{(i-1)} \begin{bmatrix} \mathbf{0}_{1\times 3} & \mathbf{Z}_i \end{bmatrix}^T \right)^{-1} \quad (12)$$

$$\breve{\mathbf{s}}^{(i)} = \breve{\mathbf{s}}^{(i-1)} + \mathbf{K}\left(\breve{a}_z^{(i)} - \begin{bmatrix} \mathbf{0}_{1\times 3} & \mathbf{Z}_i \end{bmatrix} \breve{\mathbf{s}}^{(i-1)} \right) \quad (13)$$

$$\breve{\mathbf{P}}^{(i)} = \left(\mathbf{I} - \mathbf{K} \begin{bmatrix} \mathbf{0}_{1\times 3} & \mathbf{Z}_i \end{bmatrix} \right) \breve{\mathbf{P}}^{(i-1)} \quad (14)$$

where $\breve{\mathbf{P}}^{(i)}$ is the covariance of the updated state vector after fixing the i^{th} cycle ambiguity, such that $\breve{\mathbf{P}}^{(0)} = \hat{\mathbf{P}}$. This process is repeated for the desired number of fixed ambiguities (for example *m* times). At this point, $\sigma_{v|CF}$ can be computed as the square root of the (3,3) element of $\mathbf{P}^{(m)}$, assuming that local east-north-up coordinate system is used for positioning.

$$\sigma_{v|CF} = \sqrt{\breve{\mathbf{P}}^{(m)}_{(3,3)}} \quad (15)$$

To calculate the position domain bias, we start by evaluating the impact on the state vector of fixing *m* ambiguities ($m \le n$), which is done by replacing (12) and (13) by their equivalents:

$$\begin{aligned} \mathbf{K}_m = \hat{\mathbf{P}} \begin{bmatrix} \mathbf{0}_{m\times 3} & \mathbf{Z}_{1:m\,(m\times n)} \end{bmatrix}^T \\ \left(\begin{bmatrix} \mathbf{0}_{m\times 3} & \mathbf{Z}_{1:m\,(m\times n)} \end{bmatrix} \hat{\mathbf{P}} \begin{bmatrix} \mathbf{0}_{m\times 3} & \mathbf{Z}_{1:m\,(m\times n)} \end{bmatrix}^T \right)^{-1} \end{aligned} \quad (16)$$

$$\breve{\mathbf{s}}^{(m)} = \hat{\mathbf{s}} + \mathbf{K}_m \left(\mathbf{a}^{(1:m)}_{z\,(m\times 1)} - \begin{bmatrix} \mathbf{0}_{m\times 3} & \mathbf{Z}_{1:m\,(m\times n)} \end{bmatrix} \hat{\mathbf{s}} \right) \quad (17)$$

where $\mathbf{Z}_{1:m}$ is made of rows 1 to *m* of the transformation matrix $\mathbf{Z}$. If the LAMBDA decorrelation is not used, $\mathbf{Z}_{1:m}$ is replaced by $\mathbf{Z}_{1:m} = \begin{bmatrix} \mathbf{I}_{m\times m} & \mathbf{0}_{m\times(n-m)} \end{bmatrix}$.

Assume that the correct partially-fixed ambiguity vector is $\mathbf{a}_{(m\times 1)}$ and the incorrect ambiguity vector is $\mathbf{n}_{k(m\times 1)}$. The estimated states ($\mathbf{s}_{CF}$) after fixing the ambiguities correctly and the states ($\mathbf{s}_{IF}$) after fixing the ambiguities incorrectly, respectively become:

$$\breve{\mathbf{s}}^{(m)}_{CF} = \hat{\mathbf{s}} + \mathbf{K}_m \left(\mathbf{a} - \begin{bmatrix} \mathbf{0}_{m\times 3} & \mathbf{Z}_{1:m} \end{bmatrix} \hat{\mathbf{s}} \right) \quad (18)$$

$$\breve{\mathbf{s}}^{(m)}_{IFk} = \hat{\mathbf{s}} + \mathbf{K}_m \left(\mathbf{n}_k - \begin{bmatrix} \mathbf{0}_{m\times 3} & \mathbf{Z}_{1:m} \end{bmatrix} \hat{\mathbf{s}} \right) \quad (19)$$

Therefore, the entire state error ($\mathbf{b}_k$) caused by the k^{th} incorrect ambiguity candidate vector ($\mathbf{a} - \mathbf{n}_k$) is computed by subtracting (19) from (18):

$$\mathbf{b}_k = \breve{\mathbf{s}}_{CF}^{(m)} - \breve{\mathbf{s}}_{IFk}^{(m)} = \mathbf{K}_m \left(\mathbf{a} - \mathbf{n}_k \right) \tag{20}$$

The position domain bias is then extracted from the elements in $\mathbf{b}_k$ corresponding to the position states. Then, μ_{IFk} can be determined from the vertical component of the position domain bias. We will refer to these equations later when we derive similar ones for bounding the integrity risk with a bounded measurement error.

III. Bounding Integrity Risk In the Existence of Bounded Biases

In some cases, a measurement error or fault can be bounded by a certain value due to physical limitation, data analysis, or fault monitoring. Therefore, we assume that the actual bias vector in the measurement for different satellites ($\delta\mathbf{z}$) is bounded by a vector $\mathbf{d}$ as

$$\left| \delta \mathbf{z} \right| \le \mathbf{d} \tag{21}$$

where the absolute notation here is applied on element-by-element of the vector.

This measurement error bound $\mathbf{d}$ will be used to provide a bound on the mean of the differential position estimate error. If a least squares estimator is used to estimate the position, the mean $\delta\hat{\mathbf{s}}_{|f}$ of the position estimate error can be written in terms of the pseudo inverse matrix $\mathbf{H}^+$ as,

$$\delta \hat{\mathbf{s}}_{|f} = \mathbf{H}^+ \delta \mathbf{z} \tag{22}$$

where $\mathbf{H}^+ = \left(\mathbf{H}^T \mathbf{R}^{-1} \mathbf{H} \right)^{-1} \mathbf{H}^T \mathbf{R}^{-1}$, $\mathbf{H}$ is the observation matrix and $\mathbf{R}$ is the measurement noise covariance matrix.

Using the inequality in (21), a bound $\overline{\delta \hat{\mathbf{s}}_{|f}}$ on the mean of the estimate error can be achieved as

$$\overline{\delta \hat{\mathbf{s}}_{f}} = \mathbf{H}^+ \mathbf{d} \tag{23}$$

such that $\overline{\delta \hat{\mathbf{s}}_{|f}} \ge \delta \hat{\mathbf{s}}_{|f}$.

Without cycle resolution, and by extracting the element that corresponds to the vertical component ($\overline{\delta \hat{x}_{v|f}}$) from $\overline{\delta \hat{\mathbf{s}}_{|f}}$, the vertical protection level given a bound $\mathbf{d}$ on the measurement error $VPL_{|f}$ can be computed as

$$VPL_{|f} = \overline{\delta \hat{x}_{v|f}} + K_{|f} \sigma_v \tag{24}$$

$K_{|f}$ in (24) is the integrity multiplier. Given an integrity requirement that is weighted by the fault prior probability $I_{req|f}$, $K_{|f}$ is computed using the inverse of the Gaussian cumulative distribution function Φ and $I_{req|f}$ as:

$$K_{|f} = \Phi^{-1} \left(\frac{I_{req|f}}{2} \right) \tag{25}$$

The resultant *VPL* is the maximum of the fault-free VPL (VPL_{H0}) and the faulted *VPL* ($VPL_{|f}$). Equation (24) only works for systems without cycle resolution. In the following two subsection, we provide two methods of accounting for bounded errors in the computation of protection levels or integrity risk for systems with cycle resolution.

A. Conventional Method

If cycle resolution is involved, the impact of the bias on the probability of correct fix and the impact of the fixing process on the position estimate must be taken into account. Teunissen [3] derived the impact of a bias in the cycle ambiguity estimate $\delta\mathbf{a}$ on the probability of fixing the ambiguity to any integer vector $\mathbf{n}$ as

$$P\left(\breve{\mathbf{a}} = \mathbf{n} \mid \delta\mathbf{a} \right) = \prod_{i=1}^{m} \left[\Phi\left(\frac{1 - 2\mathbf{l}_i^T \left(\mathbf{a} - \mathbf{n} + \mathbf{Z}\delta\mathbf{a} \right)}{2\sigma_{i|I}} \right) + \Phi\left(\frac{1 + 2\mathbf{l}_i^T \left(\mathbf{a} - \mathbf{n} + \mathbf{Z}\delta\mathbf{a} \right)}{2\sigma_{i|I}} \right) - 1 \right] \tag{26}$$

Therefore, the probability of correct fix given a fault can be computed by setting $\mathbf{n} = \mathbf{a}$ as

$$P_{CF|f} = P\left(\breve{\mathbf{a}} = \mathbf{a} \mid \delta\mathbf{a} \right) = \prod_{i=1}^{m} \left[\Phi\left(\frac{1 - 2\mathbf{l}_i^T \left(\mathbf{Z}\delta\mathbf{a} \right)}{2\sigma_{i|I}} \right) + \Phi\left(\frac{1 + 2\mathbf{l}_i^T \left(\mathbf{Z}\delta\mathbf{a} \right)}{2\sigma_{i|I}} \right) - 1 \right] \tag{27}$$

Therefore, if the bias on the ambiguity estimate is exactly known, (27) can be used directly to compute the probability of correct fix, which then can be used in assessing the integrity risk as shown in the previous section. However, only a bound on the ambiguity estimate bias is known by extracting the ambiguity associated elements from $\overline{\delta \hat{\mathbf{s}}_{|f}}$ (23). For the conventional method, where P_{CF} is compared to a threshold, a lower bound on $P_{CF|f}$ is used to guarantee meeting the integrity risk requirements. From (27), a lower bound on $P_{CF|f}$ can be achieved with an upper bound on $\delta\mathbf{a}$, which can be extracted from $\overline{\delta \hat{\mathbf{s}}_{|f}}$.

Next, the impact of fixing on the position estimate biases must be taken into account as well. In the process of sequentially fixing the ambiguities from float to integer numbers, not only do the cycle ambiguity states change, but the rest of the states change as well due to mutual correlation. Therefore, it is expected that the position bias due to the fault $\delta \hat{\mathbf{s}}_{|f}$ will also change. Let us write a similar expression to (18) but where the bias exists due to the fault as

$$\breve{\mathbf{s}}_{CF,f}^{(m)} = \hat{\mathbf{s}}_{|f} + \mathbf{K}_m \left(\mathbf{a} - \left[\mathbf{0}_{m\times 3} \quad \mathbf{Z}_{1:m} \right] \hat{\mathbf{s}}_{|f} \right) \tag{28}$$

In order to estimate the mean bias error, subtract (28) from (18) and write it in terms of $\delta \hat{\mathbf{s}}_{|f}$ to get

$$\delta \breve{\mathbf{s}}_{CF,f}^{(m)} = \left(\mathbf{I} - \mathbf{K}_m \left[\mathbf{0}_{mx3} \quad \mathbf{Z}_{1:m} \right] \right) \delta \hat{\mathbf{s}}_{|f} \tag{29}$$

In order to compute *VPL*, for example, let us use a vector, $\mathbf{h}_v^T$ that extracts the vertical component out of the state vector $\delta\breve{\mathbf{s}}_{CF,f}^{(m)}$ (30).

$$\delta\breve{v}_{CF,f}^{(m)} = \mathbf{h}_v\left(\mathbf{I} - \mathbf{K}_m\begin{bmatrix}\mathbf{0}_{mx3} & \mathbf{Z}_{1:m}\end{bmatrix}\right)\delta\hat{\mathbf{s}}_{|f} \tag{30}$$

Now to overbound the bias $\delta\breve{v}_{CF,f}^{(m)}$, the element-wise absolute value of $\mathbf{h}_v\left(\mathbf{I} - \mathbf{K}_m\begin{bmatrix}\mathbf{0}_{mx3} & \mathbf{Z}_{1:m}\end{bmatrix}\right)$ vector is taken and the overbound value of $\delta\hat{\mathbf{s}}_{|f}$ (which is $\overline{\delta\hat{\mathbf{s}}_{|f}}$) is used (31).

$$\overline{\delta\breve{v}_{CF,f}} = \left|\mathbf{h}_v\left(\mathbf{I} - \mathbf{K}_m\begin{bmatrix}\mathbf{0}_{m\times3} & \mathbf{Z}_{1:m}\end{bmatrix}\right)\right|\overline{\delta\hat{\mathbf{s}}_{|f}} \tag{31}$$

This bias is then used in (24) instead of $\overline{\delta\hat{x}_{v|f}}$ to compute $VPL_{|f}$. Remember that σ_v in (24) is directly influenced by the number of fixed ambiguities, which is limited by the underbound value of $P_{CF|f}$ (27) and the P_{CF} threshold.

B. EPIC Method

If we consider the integrity risk formula of EPIC (7), we notice that in order to provide a bounding integrity risk given a bounded measurement error, we have to underbound P_{CF} and P_{IFk}, and overbound $P_{VAL|CF}$ and $P_{VAL|IFk}$. Overbounding P_{CF} and underbounding $P_{VAL|CF}$ can still be achieved as was done in the conventional method (27) and (31). A similar approach can be followed for underbounding P_{IFk} and $P_{VAL|IFk}$ terms. The state vector after fixing m ambiguities given a fault f and an incorrect fix candidate $\mathbf{n}_k$ is

$$\breve{\mathbf{s}}_{IFk,f}^{(m)} = \hat{\mathbf{s}}_{|f} + \mathbf{K}_m\left(\mathbf{n}_k - \begin{bmatrix}\mathbf{0}_{m\times3} & \mathbf{Z}_{1:m}\end{bmatrix}\hat{\mathbf{s}}_{|f}\right) \tag{32}$$

Differencing (32) from (18) provides the mean in the bias due to incorrect fix $\mathbf{n}_k$ and fault f (33).

$$\delta\breve{\mathbf{s}}_{IFk,f}^{(m)} = \left(\mathbf{I} - \mathbf{K}_m\begin{bmatrix}\mathbf{0}_{mx3} & \mathbf{Z}_{1:m}\end{bmatrix}\right)\delta\hat{\mathbf{s}}_{|f} + \mathbf{K}_m\left(\mathbf{a} - \mathbf{n}_k\right) \tag{33}$$

Extracting the vertical component by multiplying (33) by the extraction vector, $\mathbf{h}_v$:

$$\delta\breve{v}_{IFk,f}^{(m)} = \mathbf{h}_v\left(\mathbf{I} - \mathbf{K}_m\begin{bmatrix}\mathbf{0}_{mx3} & \mathbf{Z}_{1:m}\end{bmatrix}\right)\delta\hat{\mathbf{s}}_{|f} + \mathbf{h}_v\mathbf{K}_m\left(\mathbf{a} - \mathbf{n}_k\right) \tag{34}$$

To overbound $P_{VAL|IFk}$, $\delta\breve{v}_{IFk,f}^{(m)}$ must be overbounded, which can be shown to be accomplished by (35).

$$\begin{aligned}\overline{\delta\breve{v}_{IFk}^{(m)}} = {} & \operatorname{sgn}\left(\mathbf{h}_v\mathbf{K}_m\left(\mathbf{a} - \mathbf{n}_k\right)\right)\left|\mathbf{h}_v\left(\mathbf{I} - \mathbf{K}_m\begin{bmatrix}\mathbf{0}_{mx3} & \mathbf{Z}_{1:m}\end{bmatrix}\right)\right|\overline{\delta\hat{\mathbf{s}}_{|f}} \\ & + \left|\mathbf{h}_v\mathbf{K}_m\left(\mathbf{a} - \mathbf{n}_k\right)\right|\end{aligned} \tag{35}$$

Underbounding P_{IFk} is not as intuitive, though. Since P_{IFk} depends on the incorrect fix candidate $\mathbf{n}_k$, the underbound will also depend on the candidate value. In other words, the maximum P_{IFk} occurs when the ambiguity bias coincide with the candidate (resulting in $\mathbf{a} - \mathbf{n}_k + \delta\mathbf{a} = \mathbf{0}$). Given a bound on $\delta\mathbf{a}$, our goal is to underbound P_{IFk}, which can be accomplished by maximizing $\mathbf{a} - \mathbf{n}_k + \delta\mathbf{a}$. Therefore, by making $\delta\mathbf{a}$ have the maximum bound and the same sign as $\mathbf{a} - \mathbf{n}_k$, we guarantee that $\mathbf{a} - \mathbf{n}_k + \delta\mathbf{a}$ is maximized, and as a result, that P_{IFk} is an underbound. In summary, an underbound on P_{IFk} is computed as

$$\begin{aligned}\underline{PIF_{k|f}} = {} & P\left(\breve{\mathbf{a}} = \mathbf{n}_k \mid \delta\mathbf{a}\right) = \\ & \prod_{i=1}^{m}\left[\Phi\left(\frac{1 - 2\mathbf{l}_i^T\left(\mathbf{a} - \mathbf{n}_k + \operatorname{sgn}\left(\mathbf{a} - \mathbf{n}_k\right)\left|\delta\mathbf{a}\right|\right)}{2\sigma_{i|I}}\right)\right. \\ & \left. + \Phi\left(\frac{1 + 2\mathbf{l}_i^T\left(\mathbf{a} - \mathbf{n}_k + \operatorname{sgn}\left(\mathbf{a} - \mathbf{n}_k\right)\left|\delta\mathbf{a}\right|\right)}{2\sigma_{i|I}}\right) - 1\right]\end{aligned} \tag{36}$$

Combining equation (27), (31), (35) and (36), an overbound on the integrity risk given a bounded on the measurement error or fault **d** can be computed using (37).

$$\begin{aligned}\overline{I_{|f}} = {} & 1 - \left(1 - \overline{P}\left\{\left|\hat{x}_v - x_v\right| > VAL \mid CF, f\right\}\right)\underline{P_{CF|f}} \\ & - \sum_{k=1}^{l}\left(1 - \overline{P}\left\{\left|\hat{x}_v - x_v\right| > VAL \mid IF_k, f\right\}\right)\underline{P_{IFk|f}}\end{aligned} \tag{37}$$

This overbounded integrity risk is then compared to the requirement $I_{req|f}$. Notice that in deriving the overbound $\overline{I_{|f}}$ in (37), we overbounded $P_{VAL|CF,f}$ and $P_{VAL|IFk,f}$ and underbounded $P_{CF|f}$ and $P_{IFk|f}$ individually. Therefore, different measurement bias values may have been selected for each one of these terms through this process. This approach, although simple and conservative, is not realistic and may provide loose bounds, as we will see in the next section. In the future, the authors will consider a more elegant approach of optimizing (37) given the bounded constraints of the measurement bias.

IV. MONTE-CARLO VALIDATION SIMULATION

In this section, we validate the methods we derived above using a Monte Carlo simulation. In this validation, we simulate one million random samples from a Gaussian distribution and then use these samples with a single satellite geometry to estimate the position. In order to present the results in the same figure, integrity risk, rather than *VPL*, is used to quantify the performance of the conventional method. This can be easily done by computing the integrity risk in (7) and (37) without taking the series term (which corresponds to incorrect fix candidates) into account. First, a fault free case without any biases is simulated and the integrity risk using the conventional method and using EPIC is compared to the actual integrity risk. The "actual" integrity risk, in this context, is computed by counting the percentage of position estimate errors that are below a certain *VAL*. To show the difference between these methods, the results are shown for different *VAL* values. Figure 1 shows the resultant integrity risk curves for the actual integrity risk and the computed integrity risk for the conventional and EPIC methods. The figure shows that both methods overbound the actual integrity risk for all values of *VAL*. Notice that due to the limited sample size of 10^6, the "actual" integrity risk curve is not meaningful statistically for values below 10^{-5}. However, EPIC provides much tighter bound to the actual integrity risk than the conventional method, because it avoids the conservative assumption that all incorrect fix candidates will cause the estimate error to exceed *VAL*. The tight bound explains the performance boost provided by EPIC in comparison with the conventional method [1].

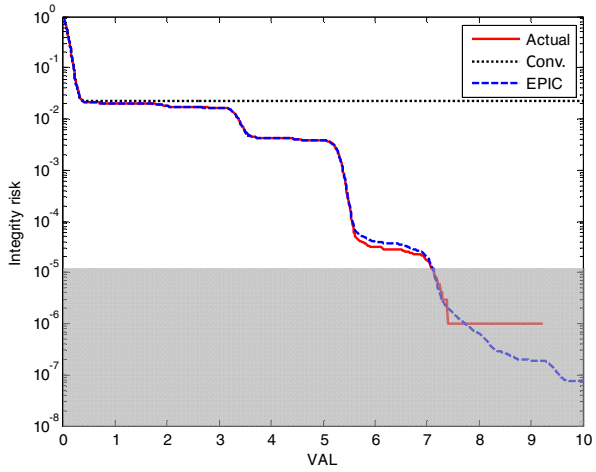

Figure 1. Integrity risk results from the Monte-Carlo Simulations for the fault free case.

In the second simulation, given a bound on the carrier phase measurement fault of 3 cm, we inject different magnitudes of the bias into the 10^6 samples and plot the actual integrity risk of each of these injected values. For the computed bound on integrity risk, only the bound on the bias is used for both the conventional and EPIC methods. In addition to the integrity risk bounds (for the conventional and EPIC methods), Figure 2 shows different curves (in red) for the different actual integrity risk corresponding to different injected bias values.

The figure shows that both bounding methods, EPIC and conventional integrity risk, do overbound the actual ones for all values of injected fault bias and all *VAL*s. EPIC, however, still provides a tighter bound than the conventional method. But, as the figure shows, EPIC bound is more conservative than the fault free case in Figure 1. This is of no surprise given that each term in (37) is bounded individually with different values of fault bias to maximize the integrity risk, which might not be realistic. If only a single value of the fault bias is allowed in maximizing (37), EPIC bound is expected to be much tighter than the one in Figure 2.

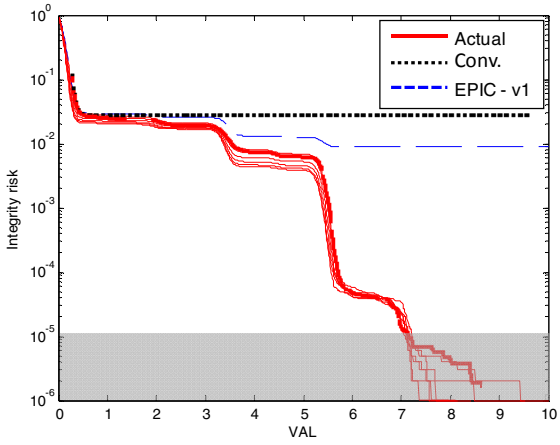

Figure 2. Integrity risk results from the Monte-Carlo Simulations for the bounded fault case.

V. Navigation Application Example

In previous work, we showed that tropospheric ducts cannot be modeled or monitored, but from extensive data analysis and post processing, a bound on the tropospheric duct error can be provided [5]. We also showed the impact of such errors on asimple navigation system that does not resolve the cycle ambiguities. Here, we demonstrate the impact of tropospheric ducting on such systems and the performance differences in using the conventional and EPIC methods.

In this section, we quantify the impact of the tropospheric duct on a high integrity and high accuracy navigation system for the application of autonomous shipboard landing. Because of the mobility of the reference station in a shipboard-relative landing application, higher levels of accuracy are required than for similar precision approach applications at land-based airfields. In addition, to ensure safety and operational usefulness, the navigation architecture must provide high levels of integrity and availability. Because of the highly stringent requirements, the navigation system is based on Carrier Phase Differential GPS (CPDGPS) positioning. However in order to benefit from the high precision of CPDGPS the cycle ambiguities must be estimated accurately. A number of methods have been used in prior work to aid in the high-integrity cycle ambiguity estimation. Satellite motion can provide the observability of the cycle ambiguities [14]. Unfortunately the rate of satellite motion is relatively slow in comparison with the time scales of the mission in considerations.

Heo, et al. have proposed a GPS navigation algorithm for autonomous shipboard landing applications where geometry-free/divergence-free code-carrier filtering is performed continuously for visible satellites on both the aircraft and the ship until the aircraft is close to the ship [15]. Geometry-free filtering [16], by definition, does not depend on the geometry of the satellites or the user location and eliminates major error sources such as atmospheric errors, clock and ephemeris errors and leaves relatively small errors such as receiver noise and multipath. A geometry free measurement of the widelane cycle ambiguity is formed by subtracting the narrowlane pseudorange from the widelane carrier [14, 16]. A drawback of the geometry free measurement is the presence of higher noise caused by the combination of L1 and L2 carrier phase measurements. This drawback can be overcome by filtering the geometry free measurement over time prior to the final approach. In order to model colored multipath noise in the geometry free measurements, a first order Gauss-Markov measurement error model is used. In this work, a time constant of one minute for the ship and 30 seconds for aircraft is assumed. The outputs of the filtering process are the floating widelane cycle ambiguity estimates. When the aircraft is close to the ship, floating L1/L2 cycle ambiguity estimates can be estimated accurately with the aid of satellite geometric redundancy [2,15,17] and are then fixed subject to the integrity risk requirements. In this work, widelane ambiguities are estimated and fixed using the geometric redundancy, instead of L1/L2.

The performance can be predicted for a single aircraft approach by covariance analysis. To account for the GPS

satellite geometry change, availability analysis is performed by simulating 1440 approaches (one approach per minute during the day). In this work, a straight in approach (Case-III landing approach) is assumed. A given approach is said to be available if the integrity requirements are satisfied at each point along the approach. Availability is calculated as the percentage of approaches for which *VPL* (in this case $VPL_{|f}$) during the entire approach is less than *VAL* and the accuracy requirement is also met (see Table I).

In this work, the requirements and simulation parameters are based on those given in [2,15,18]. The standard deviation of the raw carrier phase measurement noise is assumed to be 7 mm and the standard deviation of the raw pseudorange measurement noise is assumed to be 35 cm. Also, geometry-free prefiltering is assumed to start at the beginning of the approach and is used to generate floating estimates of the widelane cycle ambiguities. The rest of the simulation parameters are summarized in Table I. From [5], it was found that the tropospheric duct error is in the order of 6 mm. In this simulation the availability was computed for different zenith duct errors ranging from 0 to 3 cm (which encapsulates the observed 6 mm).

TABLE I. EXAMPLE SIMULATION PARANETERS

Parameter	Nominal Value
$I_{|f,req}$	6×10^{-7}
St.dev. of raw code, raw carrier	35 cm, 0.7 cm
Constellation (almanac)	24 SV (DO-229) [19]
Location	37° North, 74° West
Elevation angle mask	10°
VAL at touchdown	1.5 m
95% Instantaneous accuracy at touchdown	40 cm

Using the simulation parameters given in Table I, Figure 3 shows the impact of the tropospheric duct error using both conventional method and EPIC on an example autonomous shipboard landing navigation system. The Figure illustrates that the conventional method performance is not impressive, due to its overly conservative assumption. Availability did not exceed 78.8% event without any bounding bias. On the other hand, EPIC performs much better with availability always more than 96.6% even at 3 cm duct error bound. The figure also illustrates that the impact of the duct zenith error on availability for both approaches is similar. Varying duct zenith error bound from 0 to 3 cm reduced the availability for both approaches by 2%. However, EPIC showed the largest reduction in availability when the duct error bound increased from 1.5 cm to 3 cm. In contrast, the conventional method, suffered the same amount of availability reduction at 7 mm. The authors expect EPIC results to improve if the optimization approach, which was described in Section III.B and will be considered in the future, is implemented.

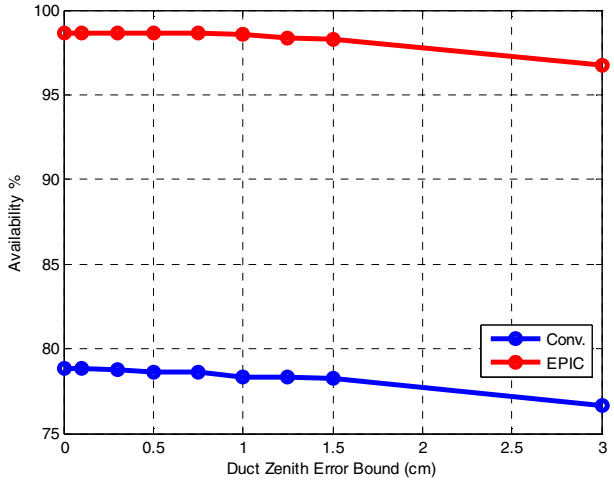

Figure 3. Availability for different values of zenith duct error bounds

VI. CONCLUSIONS

In this paper we developed a methodology to overbound the integrity risk of cycle resolution given the existence of bounded measurement errors and faults. These bounds can either represent the minimum detectable error of a fault monitor or faults or errors that cannot be detected or modeled, but which can be physically or parametrically bounded. Given fault bounds two methods to assess the integrity risk of cycle resolution were introduced and then extended to overbound the integrity risk. These methods have been verified through Monte Carlo simulations, where we highlighted the performance difference between the two. In addition, we demonstrated the usage of these methods on an example bounded error (tropospheric ducts) and an example navigation application (autonomous shipboard landing).

ACKNOWLEDGMENT

The authors gratefully acknowledge the Naval Air Systems Command (NAVAIR) of the US Navy for supporting this research. However, the opinions presented in this paper are those of the authors alone and do not necessarily represent those of NAVAIR or any other affiliated agencies.

REFERENCES

[1] S. Khanafseh and B. Pervan, "A New Approach for Calculating Position Domain Integrity Risk for Cycle Resolution in Carrier Phase Navigation Systems," IEEE Transactions on Aerospace and Electronic Systems, Vol. 46, No. 1, January 2010, pp. 296-307.

[2] S. Wu, S. Peck, R. Fries, "Geometry Extra-Redundant Almost Fixed Solutions: A High Integrity Approach for Carrier Phase Ambiguity Resolution for High Accuracy Relative Navigation," Proceedings of IEEE/ION PLANS 2008, Monterey, CA, May 2008, pp. 568-582.

[3] P. Teunissen, "Integer Estimation in the Presence of Biases," Journal of Geodesy, No. 75, 2001, pp. 399-407.

[4] M. Joerger, S. Stevanovic, S. Khanafseh, and B. Pervan, "Differential RAIM and Relative RAIM for Orbit Ephemeris Fault Detection," Proceedings of IEEE/ION PLANS 2012, Myrtle Beach, SC, April 2012.

[5] S. Khanafseh, M. Joerger, B. Pervan, and A. Von Engeln, "Accounting for Tropospheric Anomalies in High Integrity and High Accuracy

Positioning Applications," *Proceedings of the 24th International Technical Meeting of The Satellite Division of the Institute of Navigation (ION GNSS 2011)*, Portland, OR, September 2011, pp. 513–525.

[6] S. Verhagen, "The GNSS Integer Ambiguities: Estimation and Validation," Ph.D. Dissertation, Delft University of Technology, Delft, Netherlands, Jan. 2005.

[7] P. Teunissen and S. Verhagen, "The GNSS Ambiguity Ratio-test Revisited: a Better Way of Using it," Survey Review, Vol. 41, No. 312, April 2009.

[8] D. Lawrence, "A New Method for Partial Ambiguity Resolution," Proceedings of the 2009 International Technical Meeting of the Institute of Navigation ION-ITM 2009, Anaheim, CA, Jan. 2009.

[9] B. Pervan and F. C. Chan, "System Concepts for Cycle Ambiguity Resolution and Verification for Aircraft Carrier Landings," Proceedings of the 14th International Technical Meeting of the Satellite Division of the Institute of Navigation ION GPS 2001, Salt Lke City, UT, Sept. 2001.

[10] M. B. Heo, "Robust Carrier Phase DGPS Navigation for Shipboard Landing of Aircraft," Ph.D. Dissertation, Illinois Institute of Technology, Chicago, IL, Dec. 2004.

[11] S. Khanafseh, B. Kempny, and B. Pervan, "New Applications of Measurement Redundancy in High Performance Relative Navigation Systems for Aviation," Proceedings of the 19th International Technical Meeting of the Satellite Division of the Institute of Navigation ION GNSS 2006, Fort Worth, TX, Sept. 2006.

[12] P. Teunissen, "GNSS Ambiguity Bootstrapping: Theory and Application," Proceedings of KIS2001, International Symposium on Kinematic Systems in Geodesy, Geomatics and Navigation, Banff, Canada.

[13] P. Teunissen, D. Odijk, and P. Joosten, "A Probabilistic Evaluation of Correct GPS Ambiguity Resolution," Proceedings of the 11th International Technical Meeting of the Satellite Division of the Institute of Navigation, Nashville, TN, Sept. 1998.

[14] P. Misra and P. Enge, Global Positioning System signals, Measurements, and Performance. Lincoln, MA: Ganga-Jamuna Press, 2001.

[15] M. Heo, B. Pervan, S. Pullen, J. Gautier, P. Enge, and D. Gebre-Eziabher, "Robust Airborne Navigation Algorithm for SRGPS," Proceedings of IEEE/ION Position, Location, and Navigation Symposium (PLANS '2004), Monterey, CA, Apr. 2004.

[16] G. A. McGraw, "Generalized Divergence-Free Carrier Smoothing with Applications to Dual Frequency Differential GPS," NAVIGATION: Journal of Institute of Navigation, Vol. 56, No. 2, Summer 2009.

[17] S. Dogra, J. Wright, and J. Hansen, "Sea-Based JPALS Relative Navigation Algorithm Development," Proceedings of the 18th International Technical Meeting of the Satellite Division of the Institute of Navigation ION GNSS 2005, Long Beach, CA, Sept. 2005.

[18] S. Langel, S. Khanafseh, F. C. Chan, B. Pervan, "Cycle Ambiguity Reacquisition in UAV Applications using a Novel GPS/INS Integration Algorithm," Proceedings of the 2009 International Technical Meeting of the Institute of Navigation ION-ITM 2009, Anaheim, CA, Jan. 2009.

[19] "Minimum Operational Performance Standards for Global Positioning System/Wide Area Augmentation System Airborne Equipment," RTCA Document Number DO-229C, Nov. 2001, Appendix B.5.